APPRAISAL-LEVEL PREDICTION OF CANAL BREACH OUTFLOW HYDROGRAPHS

Tony L. Wahl[1], Dale J. Lentz[2], Bruce D. Feinberg[3]

Abstract: A program of physical model tests and numerical unsteady-flow simulations has been used to develop an appraisal-level tool for predicting the rate of breach development, time to peak outflow, amplitude of peak outflow, and outflow hydrograph recession time for breaching of homogeneous canal embankments. Physical model test results were used to develop relations between soil erodibility and rates of headcut advance and breach widening. These relations were consistent with previously developed relations in the literature for erosion and breaching of traditional embankment dams. Numerical studies developed separate relations for predicting breach outflow hydrograph characteristics as a function of canal hydraulic parameters, breach development rate, length of the canal pool containing the breach site, and the location of the breach relative to nearby canal check structures. A spreadsheet tool has been developed that incorporates all of these relations to predict breach outflow hydrographs as a function of embankment and canal properties. This capability will help water managers identify canal reaches and breach locations that have potential to produce large peak outflow rates. This could be used to prioritize emergency management planning activities or identify the need for additional detailed investigations. The method has not yet been tested against any real-world canal failures.

Keywords: canal failure, embankments, breaching, outflow hydrographs, hydraulic modeling

Introduction

The Bureau of Reclamation (Reclamation) is associated with more than 8,000 miles of irrigation water delivery canals in the western U.S., and failures of canal embankments have occurred periodically throughout our history. Threats to canals include animal burrows, tree roots, penetrations by turnout pipes and utilities, embankment and foundation issues, seismic events, internal erosion under static loading, hydrologic events, and operational incidents. Canal failures can have significant consequences, and the potential consequences increase as urban development surrounds formerly rural canals.

To evaluate potential consequences of a canal breach, numerical modeling of breach outflows and downstream flooding is needed. To facilitate appraisal-level investigations of Reclamation's canal inventory, a research program was established to study the canal breach process and develop tools for predicting canal breach outflow hydrographs. This work included both physical hydraulic modeling of the erosion and breaching processes and numerical modeling of transient canal behavior during a hypothetical breach event. Based on results from these studies, this paper describes a set of procedures for estimating breach initiation and breach enlargement rates and associated canal breach outflows. These procedures have been implemented in a spreadsheet model for application purposes.

[1] Hydraulic Engineer, Bureau of Reclamation, Hydraulic Investigations and Laboratory Services, Denver, CO, twahl@usbr.gov.
[2] Hydraulic Engineer, Bureau of Reclamation, Hydraulic Investigations and Laboratory Services, Denver, CO.
[3] Hydraulic Engineer, Bureau of Reclamation, Flood Hydrology and Emergency Management, Denver, CO.

Background

Although canal breaches have occurred throughout history, there have been remarkably few efforts to generalize experiences from these events. Prior to this study, there was no guidance specific to canals for predicting breach parameters or breach outflow hydrographs. Dun (2007) provided the most notable prior work on the hydraulics of a canal breach in a study of a navigation canal that failed in the United Kingdom in 2004. Dun concluded that the hydraulics of canal breaches were significantly different from breaches of traditional dams and storage reservoirs. For a traditional dam breach, outflow is typically limited by the breach geometry and the reservoir storage, but for a canal breach, outflow is also limited by the conveyance capacity of the canal reaches that deliver water to the breach site.

Nearly all canal embankments contain soils that will support headcut development during erosion. Even canal embankment soils that do not exhibit plasticity contain enough fines to resist seepage loss of water and thus exhibit enough apparent cohesion that headcuts can develop. Recognizing this general characteristic, the typical stages of a canal breach can be described as follows:

1. Initial overtopping of the embankment, or development of a defect in an embankment that allows erosive flow through the embankment or foundation (piping).

2. Development of a headcut that begins on the downstream (outer) slope of the embankment and migrates upstream toward the canal. In this stage, erosion is primarily taking place downstream from the section that controls the outflow rate (the hydraulic control). The breach outflow rate is small and normal canal flow is maintained past the developing breach site.

3. Migration of the headcut through the hydraulic control, which enlarges the control section rapidly and allows a dramatic increase in outflow. As the breach enlarges, the size of the breach and the water level maintained in the canal are the primary factors determining the outflow rate. In this phase, the breach outflow becomes so large that flow reverses in the canal reach that was initially downstream from the breach site.

4. The breach eventually enlarges to the point that the hydraulic control shifts from the breach to the two canal sections. Critical-depth flow occurs in the leg of the canal upstream from the breach and also in the leg of the canal downstream from the breach. The breach may continue to widen, but the outflow rate cannot increase. As the canal drains, the outflow rate begins to reduce.

One potential modification of this staged breach process is a situation in which the embankment is weak enough to allow the overtopping channel or initial pipe to enlarge rapidly enough that steps 2 and 3 are not distinct from one another but are effectively combined into one step. This would not change the hydraulic control shift that still occurs during the last step of the process.

The research studies carried out at Reclamation have focused on the last 3 steps of the process outlined above. These studies have assumed that the occurrence of the first step in

the process is given; there has been no attempt to model the initiation of piping. These studies have also been based on the conservative assumption that there is no intervention in the process as described, such as early shutdown of the canal or closing of check gates at the upstream and downstream ends of a reach experiencing a breach event. This provides results that are appropriate for the worst-case scenario of a breach that develops so rapidly that intervention is not possible.

Physical Modeling

Physical modeling to support this research was described in detail by Wahl et al. (2011). The facility used in the hydraulics laboratory (Figure 1) recreated a typical canal flow situation prior to development of a breach. Water could be provided into both ends of a non-erodible canal with an erodible test section in the middle. Each test started with normal canal flow past the test embankment, and as the breach developed, the flow into both ends of the model canal was increased to maintain boundary conditions at the breach site that were representative of a fast-developing breach in a long canal reach (i.e., a relatively steady canal water surface). The upper limit of inflow to each end of the canal was the theoretical critical-flow discharge capacity of the canal sections.

Figure 1. — Overview of canal breach model test facility, looking in the upstream direction.

The three tested embankments were constructed in the model as simulated fill sections in a canal reach that is elevated above the surrounding landscape. Soil used to construct the embankments was a silty sand (SM) obtained from a local landscape materials supplier. To simulate the wide range of erodibility properties that can occur in real canal embankments, we varied both the water content at compaction and the level of compaction effort. The test soil

contained about 10% clay fines and exhibited some plasticity (PI=5), so its erodibility was sensitive to the placement conditions. Across three breach tests, the erodibility of the embankments varied by about three orders of magnitude as indicated by detachment rate coefficients measured in submerged jet tests conducted with ASTM D5852 procedures (Hanson and Cook 2004).

The tests exhibited three canal breach development scenarios, all initiated by erosion through a pre-formed pipe in the embankment (a #4 rebar embedded in the embankment and removed to start the test). The first test with a well-compacted and erosion-resistant embankment produced a very slow headcut migration and breach widening process, without a sudden and catastrophic breach outflow. This test was representative of a real situation in which there would likely be adequate time to shut down the canal and reduce the severity of the breach outflow. The second test demonstrated the breach behavior of a poorly-compacted and very erodible embankment, with rapid headcut development, headcut migration, and breach widening. The third test illustrated an intermediate situation in which the embankment was very erodible, but the initial pipe was located so high in the embankment that flow through it was small and headcut development and migration were slow. However, when the headcut finally migrated into the canal prism, failure and breach widening were nearly as rapid as that seen in the second test.

Data collected from the three tests were used to relate soil erodibility parameters (detachment rate coefficient and critical shear stress) and hydraulic attack (estimated shear stresses and energy dissipation rates) to observed headcut migration and breach widening rates. The relations between these variables were found to be consistent with observations from breach testing of traditional embankment dams (Hunt et al. 2005; Temple et al. 2005; Hanson et al. 2011). This led to the development of simplified mathematical models for predicting headcut advance, piping hole enlargement, and breach widening rates. The first two models are relevant to estimating the time required for *breach initiation*, which affects the amount of time available for detection of a breach in progress and warning of the downstream population at risk. The last model can be used to estimate the rate of breach enlargement.

Numerical Modeling

If the ultimate breach width and breach widening rate can be estimated, the next challenge is to estimate the breach outflow hydrograph that would be produced. This is dependent on both the characteristics of the breach and the transient behavior of the canal reach in which the breach occurs, since drawdown of the canal and development of a varying water surface profile in the canal will change the head acting on the breach opening and the amount of flow that can be delivered to the breach site. To quantify these effects, one-dimensional unsteady flow modeling was undertaken using HEC-RAS (Wahl and Lentz 2011; Wahl 2012). Numerous canal breach scenarios were simulated with varying canal sizes, breach times, canal reach lengths, and breach locations within the canal reach. This led to the development of dimensionless relationships that yield estimates of breach hydrograph parameters (peak outflow and recession time) as a function of breach development time, breach location within the canal reach, and canal hydraulic properties.

Canal Breach Outflow Prediction Procedure

The essential characteristics of a canal breach hydrograph are the time required for breach initiation, the time required for breach development, and the resulting breach outflow hydrograph. The hydrograph may be defined by the peak outflow magnitude, the time at which peak outflow occurs, and the time required for the hydrograph to recede. The physical embankment breach tests and HEC-RAS modeling conducted in this research project provide a basis for estimating all of these characteristics of a canal breach event.

Breach Initiation

Breach initiation may take place through one or a combination of three different processes: headcut advance caused by overtopping flow; headcut advance due to flow through an existing piping channel that is not enlarging significantly; or direct erosion and enlargement of an existing piping defect. Models for all three processes are presented, although those based on headcutting are believed to be more reliable at this time.

Breach Initiation by Headcut Advance due to Overtopping Flow

Consider the canal embankment shown in Figure 2, which is depicted as a fill section deeper than the canal prism. Flow overtops the embankment with head H_{ov}. The unit discharge over the embankment can be estimated from a broad-crested weir equation as $q=2.6H_{ov}^{1.5}$ with H_{ov} in ft and q in $ft^3/s/ft$. (For metric units of m and $m^3/s/m$ the coefficient 2.6 $ft^{1/2}/s$ becomes 1.44 $m^{1/2}/s$.) Assuming that headcutting initiates at the toe of the embankment, the time for breach initiation is the time required for the headcut to advance the distance L back to the upstream edge of the embankment crest. The headcut advance rate can be estimated from (Temple et al. 2005)

$$\frac{dX}{dt} = C\left(qH_h\right)^{1/3} \tag{1}$$

where:

dX/dt = headcut advance rate (ft/hr);
C = headcut advance rate coefficient ($s^{1/3}/hr$);
q = unit discharge ($ft^3/s/ft$); and
H_h = headcut height (ft).

Hanson et al. (2011) showed (and our physical hydraulic model testing of canal breaches confirmed) that C can be estimated as $C=0.44k_d$, with k_d being the detachment rate coefficient obtained from a submerged jet erosion test with units of ft/hr/psf. (If k_d is given in metric units of $cm^3/(N\text{-}s)$, then $C=0.25k_d$ and the units of C remain the same.) In the event that a jet test is unavailable, values of k_d may be estimated using Table 1 (Hanson et al. 2011) which relates k_d to the clay content, compaction effort, and water content of the soil during compaction.

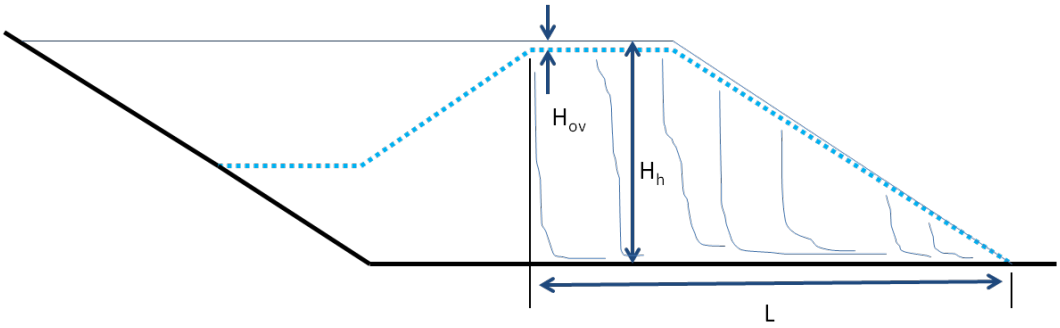

Figure 2. — Canal embankment parameters for estimating headcut advance rate due to overtopping flow.

Combining these equations together, the time for breach initiation in hours is:

$$t_{\text{initiation}} = \frac{L}{\left(0.44k_d\right)\left(2.6H_{\text{ov}}^{1.5}H_h\right)^{1/3}} \tag{2}$$

where:

L = required headcut advance distance, from toe of exterior slope (ft);
H_h = potential height of headcut (ft);
H_{ov} = overtopping head (ft); and
k_d = detachment rate coefficient (ft/hr/psf).

One could argue that the headcut should be assumed to initiate at the top of the slope to conservatively shorten the migration distance required, but in that case the head acting on the headcut would be initially small. The headcut would eventually deepen to approach H_h, and it is believed that the time required for this to occur is comparable to the time needed for headcut migration from the toe back to the head of the slope.

Table 1. — Approximate values of k_d in cm^3/(N-s) as a function of compaction conditions and % clay (Hanson et al. 2011). [1 cm^3/(N-s) = 0.5655 ft/hr/psf]

% Clay (<0.002 mm)	Modified Compaction (56,250 ft-lb/ft^3)		Standard Compaction (12,375 ft-lb/ft^3)		Low Compaction (2,475 ft-lb/ft^3)	
	≥Opt WC%	<Opt WC%	≥Opt WC%	<Opt WC%	≥Opt WC%	<Opt WC%
	Erodibility, k_d, cm^3/(N·s)					
>25	0.05	0.5	0.1	1	0.2	2
14-25	0.5	5	1	10	2	20
8-13	5	50	10	100	20	200
0-7	50	200	100	400	200	800

Breach Initiation by Headcut Advance due to Piping Flow

Analysis of this case is similar to the previous situation, except that the overtopping flow is replaced by orifice flow through a piping defect in the embankment. The elevation of this defect and its diameter and length must be specified to allow estimation of the flow rate

through the pipe. The starting diameter should be a practical value relating to the size of piping defect that might prompt notice of the piping condition by project personnel and begin the cycle of potential operational responses to a canal emergency. The key variables are illustrated in Figure 3.

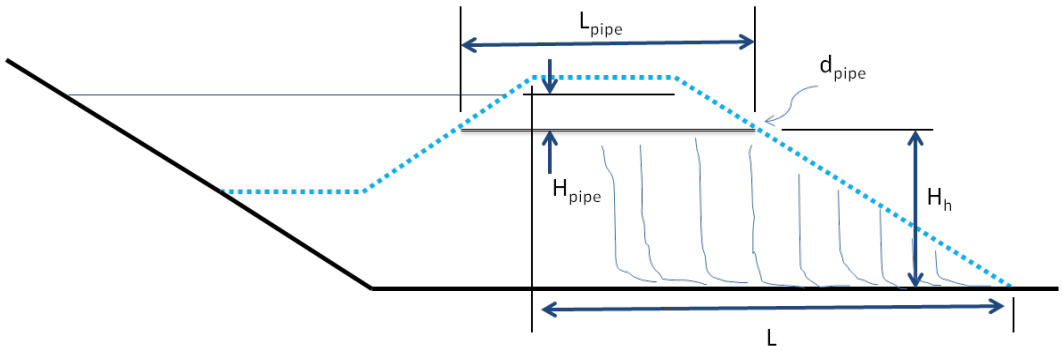

Figure 3. — Canal embankment parameters for estimating headcut advance rate due to piping flow.

The flow rate through the pipe can be estimated by applying the energy equation

$$Q = \frac{\pi\left(d_{\text{pipe}}\right)^2\sqrt{2gH_{\text{pipe}}}}{4\sqrt{1+f\dfrac{L_{\text{pipe}}}{d_{\text{pipe}}}}} \tag{3}$$

where:

Q = discharge (ft^3/s);
d_{pipe} = pipe diameter (ft);
g = acceleration due to gravity (ft/s^2);
H_{pipe} = head across pipe (ft);
f = friction factor, assumed to be 0.05 for a relatively rough pipe interior; and
L_{pipe} = length of pipe (ft).

The unit discharge effective in advancing the headcut can then be estimated by converting the flow through the round pipe into the unit discharge of an equivalent square jet, $q=(\pi/4)^{1/2}(Q/d_{\text{pipe}})=0.886Q/\text{d}_{\text{pipe}}$. The time required for headcut advance is then computed as

$$t_{\text{initiation}} = \frac{L}{\left(0.44k_d\right)\left(0.886QH_h/d_{\text{pipe}}\right)^{1/3}} \tag{4}$$

Note that the distance L is shown in Figure 3 as the distance to the upstream crest, not the full distance to the upstream end of the pipe. This leads to a shorter, more conservative estimate of the breach initiation time and is consistent with the observed behavior of the test embankments, which seemed to experience collapse of the bridge over the pipe at about the time that headcutting reached the upstream side of the crest.

Breach Initiation by Pipe Enlargement

A model for pipe enlargement was developed by Wahl and Lentz (2011), but was extremely sensitive to the values of k_d and the critical shear stress of the soil, τ_c, as well as the choice of a starting condition for the piping erosion analysis. In erosion resistant materials, the model may predict a very long time to reach breach initiation, and headcut advance due to the piping flow will probably be found to breach the embankment much more quickly. In very weak materials, this model may predict a very rapid breach, but it is likely that the headcut advance model would also predict a very rapid breach for those conditions. This model is presented here primarily for its potential value in further research. If piping is to be analyzed, the model for headcut advance driven by the piping flow is recommended for practical use at this time.

To analyze pipe enlargement, a starting diameter for the pipe must be selected. As discussed in the previous section, this should be a practical value relating to the size of piping defect that might prompt notice of the piping condition by project personnel and begin the cycle of potential operational responses to a canal emergency. With the pipe diameter and its length specified, the initial flow rate through the pipe, Q_0, can be estimated with Eq. 3. The initial shear stress through the pipe can be estimated as

$$\tau_0 = \frac{\gamma_w S d_{\text{pipe}}}{4} \tag{5}$$

where:

γ_w = unit weight of water, and
S = hydraulic gradient acting on the pipe.

The erosion time scale, t_{er}, can be estimated as

$$t_{er} = \frac{2L_{\text{pipe}}}{k_d \gamma_w H_{\text{pipe}}} \tag{6}$$

The value of the detachment rate coefficient, k_d, for this model should come from a hole erosion test (Wan and Fell 2004). Wahl et al. (2008) studied the hole erosion test and the submerged jet test and found significant differences in the detachment rate coefficients and critical shear stresses produced by the two tests. If k_d is only available from a submerged jet test, then the value should be reduced by a factor of 10.

Once the erosion time scale has been determined, the flow rate $Q(t)$ at any time t can be computed using a parametric model based on the initial discharge, Q_0, initial shear stress, τ_0, and critical stress parameter for the soil, τ_c.

$$t = t_{er} \ln\left(1 + \frac{\left(Q(t)/Q_0\right)^{2/5} - 1}{1 - \tau_c/\tau_0}\right) \tag{7}$$

The critical shear stress, τ_c, should be obtained from a hole erosion test, or the result from a jet test may be used if increased by a factor of 100. Although τ_c values for many weak

materials are believed to be practically zero for use in many erosion modeling equations, a non-zero value should be considered for this analysis, otherwise the denominator in Eq. 7 is simply 1. For this purpose, Table 2 is suggested.

Table 2. — Approximate values of τ_c in Pa as a function of compaction conditions and %clay (modified from Hanson et al. 2010). These values of τ_c are representative of submerged jet test results. For use in the piping erosion model (Eq. 7), they should be increased by a factor of 100. [1 Pa = 0.0209 psf]

% Clay (<0.002 mm)	Modified Compaction (56,250 ft-lb/ft^3)		Standard Compaction (12,375 ft-lb/ft^3)		Low Compaction (2,475 ft-lb/ft^3)	
	≥Opt WC%	<Opt WC%	≥Opt WC%	<Opt WC%	≥Opt WC%	<Opt WC%
	Critical shear stress, τ_c, Pa					
>25	16	0.16	4	0.04	1	0.01
14-25	1.6×10^{-1}	1.6×10^{-3}	4×10^{-2}	4×10^{-4}	1×10^{-2}	1×10^{-4}
8-13	1.6×10^{-3}	1.6×10^{-5}	4×10^{-4}	4×10^{-6}	1×10^{-4}	1×10^{-6}
0-7	1.6×10^{-5}	1.0×10^{-6}	4×10^{-6}	2.5×10^{-7}	1×10^{-6}	6×10^{-8}

A suggested condition defining the end of breach initiation and a transition to the breach development phase is based upon the discharge through the piping hole, $Q(t)$ equal to 5% of the normal canal discharge. The elapsed time required will be found to be relatively insensitive to the specific percentage of canal flow selected, as the discharge through the piping hole increases rapidly near the end of the breach initiation process. Eq. 7 will only be valid for $\tau_c<\tau_0$ and $Q(t)>Q_0$.

Breach Development

The breach development phase is characterized by headcut advancement through the upstream (canal side) slope of the embankment down to its toe, followed by widening of the breach in both directions until the breach becomes wide enough that it no longer serves as the hydraulic control. At this point, control of the flow shifts to the critical-flow sections that will exist in the upstream and downstream canals. For purposes of this appraisal-level model, the period of headcut advance into the canal is assumed to be short compared to the time for breach widening and is incorporated into the estimate of the widening time by assuming that widening begins from a breach width of zero. The breach will be assumed to have vertical sidewalls during the widening phase and a rectangular cross-section, as observed in physical model tests and real embankment failures.

To estimate the breach development time, it will be necessary to first define the ending condition for this phase. We need to determine the maximum theoretical flow that can be provided to the breach site by the upstream and downstream canals. This is accomplished by iteratively solving a system of three equations applying to critical flow (Clemmens et al. 2001):

$$Q = \sqrt{\frac{gA_c^3}{T_c}} \tag{8}$$

$$y_c = H_1 - \frac{A_c}{2T_c} \tag{9}$$

$$H_1 = h_1 + \frac{Q^2}{2gA_1^2} \tag{10}$$

where:

y_c = *critical depth,*
A_c = area of the critical section,
T_c = top width of the critical section,
h_1 = normal flow depth in the canal,
H_1 = total energy head in the canal at normal flow, and
A_1 = area of the canal at normal depth.

For the design normal-depth flow condition of the canal, the flow depth h_1 is known and a value of H_1 can be computed using Eq. 10. Next, assume a starting value for critical depth, y_c, such as y_c=0.7H_1. For this critical depth, the cross-sectional area, A_c, and top width, T_c, of the canal may be computed. The critical discharge can then be computed from Eq. 8 and a refined estimate of y_c computed with Eq. 9. H_1 should be kept constant, so the iteration between Eqs. 7 and 8 is continued until convergence is obtained. The maximum theoretical breach outflow, $Q_{c,max}$, will then be two times the critical discharge computed with Eq. 8, assuming that both canals have the same cross section. The critical flow depth through the rectangular breach opening will then be estimated as (2/3)y_n, where y_n is the normal depth of flow in the canal. For a rectangular channel, the critical flow depth is y_c=(q^2/g)$^{1/3}$, so the unit discharge at the end of breach widening is q=([2y_n/3]^3g)$^{1/2}$ and the final width of the breach is

$$b_{\max} = \frac{Q_{c,\max}}{\sqrt{\left(\frac{2y_n}{3}\right)^3 g}} \tag{11}$$

The breach widening rate is estimated using a relation developed by Hunt et al. (2005) and confirmed in the physical model tests discussed previously.

$$\frac{db}{dt} = 2k_d[0.7\gamma_w g(y_c^{1/3} n/1.49)^2 - \tau_c] \tag{12}$$

where *db/dt* is the change in breach width per unit time, the constant 1.49 comes from the Manning equation in English units, and Manning's *n* is taken to be 0.020 in the breach opening. With the final breach width and widening rates known, the time required for breach widening is

$$t_f = \frac{b_{max}}{2k_d[0.7\gamma_w g(y_c^{1/3} n/1.49)^2 - \tau_c]} \quad (13)$$

If desired, the critical shear stress, τ_c, may be assumed to be zero to obtain a conservatively shorter estimate of the breach widening time. Once the breach widening time is estimated, it is converted to a dimensionless quantity, $t^*_f = t_f/t_{ref}$, with t_{ref} being a reference time based on the hydraulic depth of the canal, D, and the wave celerity, c

$$t_{ref} = \frac{D}{c} = \frac{D}{\sqrt{Dg}} = \sqrt{D/g} \quad (14)$$

In this equation the hydraulic depth, D, is equal to the canal flow area divided by the wetted top width, and g is the acceleration due to gravity.

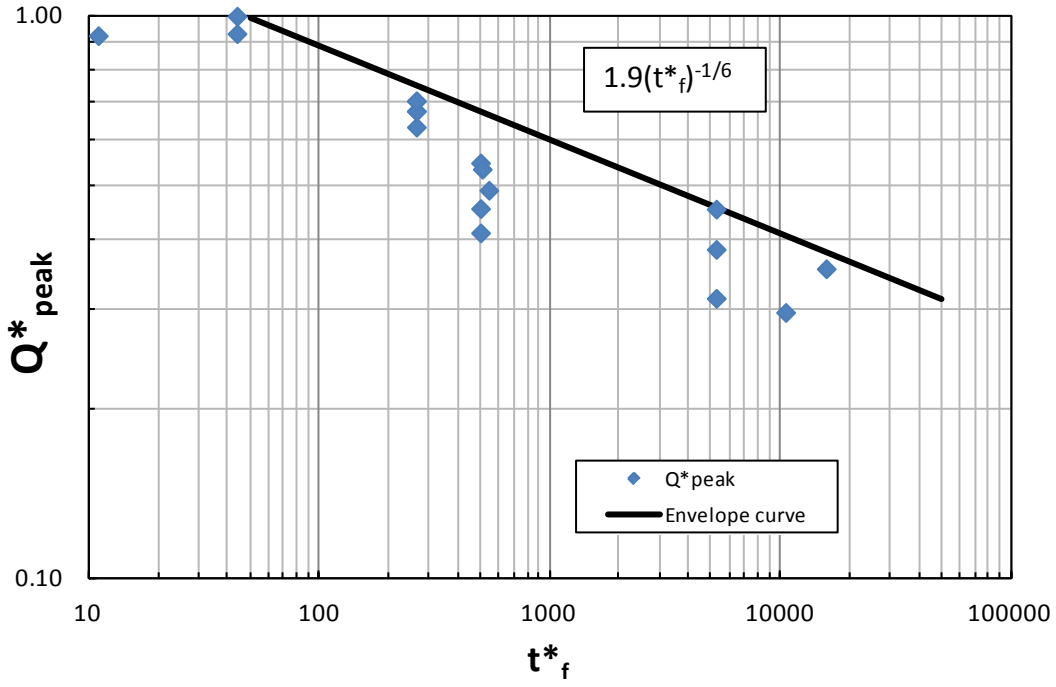

Figure 4. — Dimensionless peak outflow from hypothetical canal breaches as a function of dimensionless breach development time.

Previous numerical modeling of hypothetical canal failures (Wahl and Lentz 2011; Wahl 2012) developed relations for predicting the dimensionless peak outflow, $Q^*_{peak} = Q_{peak}/Q_{c,max}$. Figure 4 shows the dimensionless peak outflow versus the dimensionless breach development time. Data points at or just below the upper envelope curve come from simulations in which the hypothetical breach site is a long distance upstream from the next downstream check structure along the canal, so there is a significant volume of water in the downstream canal that can drain back upstream to add to the breach outflow. Points lying well below the envelope curve are for simulations in which the breach site was closer to the downstream end of the canal reach. Figure 5 shows the percentage of the envelope value that was actually developed as a function of the dimensionless distance from the breach site to the downstream end of the reach. Note that the curve shown in Figure 5 is modified from that shown in the

previous references so that the curve passes through 50% at a dimensionless distance of 1. Thus, if the breach is located very near the downstream end of the reach, then the downstream channel is short and contributes almost nothing to the peak outflow, so the maximum possible outflow is 50% of the value obtained from the envelope curve. Note also that in the numerical simulations the distance from the breach to the upstream end of the canal reach had much less effect on the peak outflow than did the downstream distance. Combining the two relations shown on these figures produces one equation for estimating the peak outflow:

$$Q_{\text{peak}} = Q_{c,\max}(Q^*_{\text{peak}}) = Q_{c,\max}\frac{1.9}{(t^*_{\text{f}})^{1/6}}\left[1-\frac{0.5}{(L^*_{\text{ds}})^{1/4}}\right] \quad (15)$$

where t^*_{f} is the dimensionless breach development time (breach widening time) divided by the time scale reference, $t_{\text{ref}}=(D/g)^{0.5}$, and L^*_{ds} is the downstream canal reach length nondimensionalized by the hydraulic radius, L_{ds}/R_h.

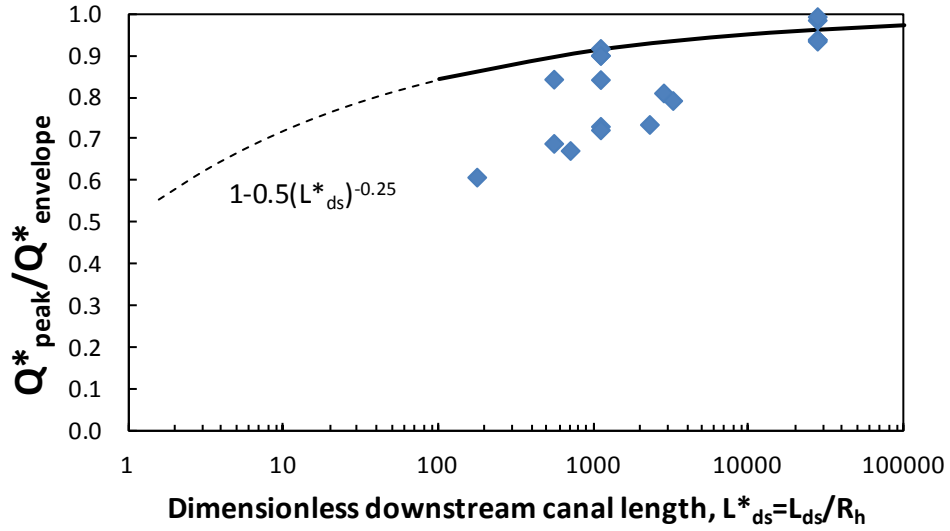

Figure 5. — Effect of downstream canal reach length on peak breach outflow. L_{ds} is the length of the downstream canal and R_{h} is the hydraulic radius.

The peak discharge can be assumed to occur at the end of the breach widening phase. The other parameter of significant interest is the time required for the breach outflow to recede back toward the normal canal flow rate. (Since we assume that the canal is not shut down during a hypothetical "fast" breach, the canal continues to supply water from upstream at the normal rate.) To describe the recession curve, the duration for the flow to drop back to a flow rate of $Q_{\text{normal}}+0.5(Q_{\text{peak}}-Q_{\text{normal}})$ can be estimated with Eq. 16 (Wahl and Lentz 2011), which defines the curve shown in Figure 6.

$$t_{\text{recession}} = \frac{123}{t^{*0.66}_{\text{f}}}t_{\text{f}} \quad (16)$$

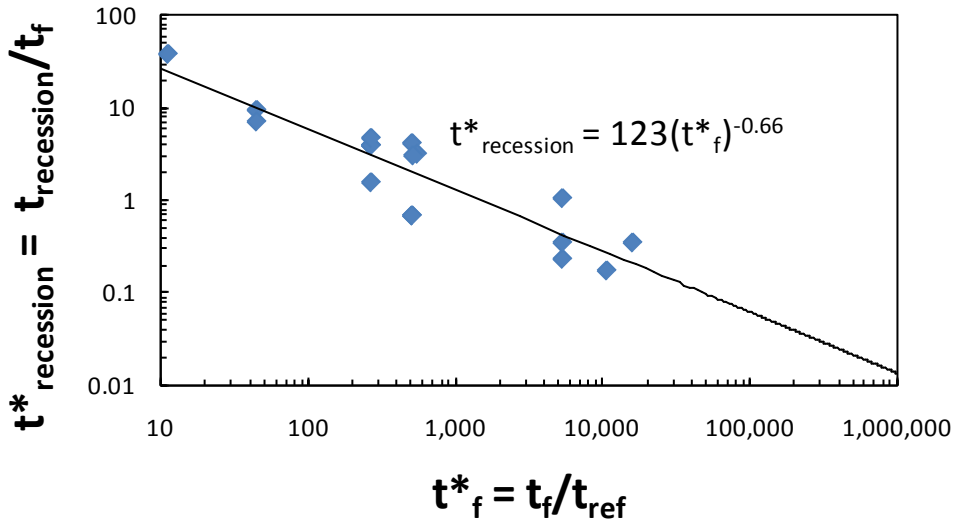

Figure 6. — Hydrograph recession time as a function of breach development time.

Spreadsheet Model

The set of equations described above has been programmed into a spreadsheet model that allows a user to describe the canal properties, the embankment dimensions, and the embankment materials, and then estimate breach initiation time, breach development time, and the breach outflow hydrograph. The next step in the development of this tool is to validate it against actual canal failures. This will require case studies with the necessary input data and good estimates of the actual breach outflow hydrograph.

Conclusions

Prediction of canal breach outflow hydrographs requires modeling of both breach development processes and the transient response of the canal. Physical model testing and analytical work has produced methods for estimating breach initiation time, breach development time and breach width. Numerical modeling of canal and breach dynamics has produced relations for predicting breach outflow hydrograph characteristics as a function of breach development time and breach location within a canal pool relative to nearby check structures that regulate the canal flow. These components have been assembled to create an integrated mathematical model that can be used to make appraisal-level estimates of canal breach outflow hydrographs as a function of canal hydraulic properties and embankment material properties. The method has not yet been tested against any real-world canal failures.

References

1. ASTM, 2003. Annual Book of ASTM Standards, Section 4: Construction, Vol. 04.08. Philadelphia, Pa.: ASTM.
2. Dun, R.W.A., 2007. An improved understanding of canal hydraulics and flood risk from breach failures. *Water and Environment Journal.* 21(1): 9-18.
3. Hanson, G.J., and K.R. Cook, 2004. Apparatus, test procedures, and analytical methods to measure soil erodibility *in situ*. *Applied Engineering in Agriculture*, 20(4):455-462.

4. Hanson, G.J., D.M. Temple, S.L. Hunt, and R.D. Tejral, 2011. Development and characterization of soil material parameters for embankment breach. *Applied Engineering in Agriculture*, 27(4):587-595.
5. Temple, D.M., G.J. Hanson, M.L. Neilsen, and K.R. Cook. 2005. Simplified breach analysis for homogeneous embankments: Part 1. Background and model components. In *Technologies to Enhance Dam Safety and the Environment*, Proceedings of the Annual Meeting of the United States Society on Dams, Denver, Colorado, 151-161.
6. Wahl, T.L. and D.J. Lentz, 2011. *Physical hydraulic modeling of canal breaches,* Hydraulic Laboratory Report HL-2011-09, U.S. Dept. of the Interior, Bureau of Reclamation, Denver, CO.
7. Wahl, T.L., D.J. Lentz, and B.D. Feinberg, 2011. Physical hydraulic modeling of canal breaches*,* In: *Dam Safety 2011*, Annual Meeting of the Association of State Dam Safety Officials (ASDSO), Sept. 26-29, 2011, Washington, DC.
8. Wahl, T.L., 2012. Numerical modeling to predict canal breach outflow hydrographs. 2012 World Environmental and Water Resources Congress, Environmental and Water Resources Institute of the American Society of Civil Engineers, Albuquerque, NM, May 20-24, 2012.